Water Air Soil Pollut (2026) 237:627
https://doi.org/10.1007/s11270-026-09300-y

Optimization of Sustainable Hybrid Natural–Waste Adsorbent Compositions for Mixed Dye Removal from Aqueous Solutions

Sevgi Fersiz · Melike Isgoren · Erhan Gengec · Suna Demir

Received: 30 October 2025 / Accepted: 20 February 2026
© The Author(s) 2026

Abstract In this study, the removal of a synthetic dye mixture containing anionic (Telon Blue AGLF), cationic (Astrazon Blue BG-200%), and nonionic (Dianix Blue S-BG) dyes from aqueous solutions was investigated using the adsorption method. As an alternative to commonly used commercial adsorbents, three low-cost, naturally abundant, and renewable materials magnolia cone (MC), beidellite (BD), and fly ash (FA) were selected. Unlike many previous studies in the literature, these adsorbents were used simultaneously to explore the potential advantages of combined adsorption. Batch adsorption experiments were conducted by varying the operational parameters, including pH (4–11), contact time (5–60 min), and the individual dosages of three different adsorbents (within the range of 0.01–0.04 g), while keeping the initial dye concentrations constant. A synthetic dye solution was prepared by mixing the three dyes in equal concentrations and volumes. The effects of the selected parameters on dye and total organic carbon (TOC) removal efficiencies were evaluated and optimized using Response Surface Methodology (RSM) based on Central Composite Design (CCD). To assess the structural and surface characteristics of the adsorbents before and after adsorption, Brunauer–Emmett–Teller (BET) surface area analysis and Scanning Electron Microscopy (SEM) were employed. BET analysis revealed surface areas of the adsorbents ranging from 18 to 158.5 m^2/g. SEM images demonstrated that dye molecules were successfully adsorbed onto the surface and within the pores of the adsorbents. The findings indicate that the simultaneous use of natural and waste-derived materials can offer a sustainable, efficient, and cost-effective approach for the removal of mixed dyes from wastewater.

Keywords Adsorption · Dyestuff removal · Magnolia cone · Beidellite · Fly ash · Central Composite Design

1 Introduction

Dyes are extensively utilized as coloring agents in various industries, including textiles, pharmaceuticals, plastics, cosmetics, food, leather, photography and paper (Nath et al., 2025). Dyes are considered one of the primary and persistent pollutant groups in industrial wastewater, posing significant challenges for conventional treatment processes in environmental engineering (Wei et al., 2025). Industrial activities are responsible for the production of approximately 700,000 tons of dyes annually, with an estimated 280,000 tons ultimately entering receiving waters as waste (Abdulhameed et al., 2025a). The release of organic dyes into aquatic environments reduces water quality by limiting oxygen availability and light

S. Fersiz · M. Isgoren (✉) · E. Gengec · S. Demir
Department of Environmental Protection, Kocaeli University, 41275 Izmit, Türkiye
e-mail: melike.isgoren@kocaeli.edu.tr

Published online: 03 March 2026

penetration, adversely affecting aquatic life. Moreover, certain dyes and their degradation products are mutagenic, carcinogenic, or toxic, posing risks to human health and potentially contaminating drinking water and the food chain (Abdulhameed et al., 2025b). Therefore, it is essential to ensure that wastewater is effectively treated prior to discharge, and that dye residues are safely disposed of into any water body in compliance with national and international standards (Solayman et al., 2023).

Dyes used in various industries can be classified in many ways depending on their color characteristics, chemical structures, and application areas. In the present study, dyes are categorized into three main types cationic**,** anionic, and neutral dyes based on their electrical charge when dissolved in aqueous media. Specifically, cationic dyes carry a positive charge, anionic dyes possess a negative charge, whereas neutral dyes exist as electrically uncharged molecules in solution (Jha et al., 2025; Shi et al., 2022). Due to their positively charged nature, cationic dyes are classified as basic dyes, whereas anionic dyes with negative charges include direct, acid, and reactive dyes (Salleh et al., 2011). Wastewater often contains not a single dye, but a mixture of dyes with varying charges, molecular structures, and chemical properties. This creates a complex, multi-component matrix, the treatment of which poses a significant global challenge (Jha et al., 2025). Various methods have been explored for the elimination of dyes from wastewater, including chemical and electrochemical coagulation, flocculation, ion exchange, membrane filtration, advanced oxidation techniques, adsorption, photocatalysis, and photooxidation (Daneshvar et al., 2017; Khan et al., 2023; Solayman et al., 2023). Among these methods, adsorption offers significant application potential due to its advantages, including low cost, minimal energy requirements, safety, efficiency, and operational simplicity (Shao et al., 2025). Various adsorbents have been effectively employed for the removal of dyes from wastewater. Activated carbons are widely used due to their high surface area and extensive porosity, and their adsorption capacity can be further enhanced through chemical activation. Biochars derived from agricultural residues provide a low-cost and environmentally sustainable alternative. Clays and minerals are particularly effective for cationic dyes and their capacity can be improved through suitable modifications. Polymeric adsorbents (e.g., chitosan) offer selective adsorption and reusability advantages, although their production costs are higher. Moreover, nanomaterials and composites demonstrate significant potential for industrial applications due to their high surface area and ease of recovery. The performance of these adsorbents is directly related to surface area, porosity, and functional group density, while the adsorption mechanisms generally involve electrostatic interactions, hydrogen bonding, and π–π interactions. Selecting the appropriate adsorbent for different dye types is critical for achieving optimal adsorption capacity and efficiency (Abdulhameed et al., 2025b; Gengec et al., 2018; Isgoren, 2024; Isgoren et al., 2025; Wei et al., 2025). Despite their effectiveness, activated carbons are associated with high treatment and regeneration costs, and are sometimes used as single-use materials. Their disposal may contribute to secondary pollution, thereby emphasizing the need for cost-effective natural or synthetic alternative adsorbents (Mokhtar et al., 2024).

Biosorption has emerged as a cost-effective and environmentally friendly approach for the removal of contaminants from wastewater, particularly those that are not easily biodegradable, such as dyes. Both living and non-living organisms, including bacteria, fungi, algae, and yeasts, as well as agricultural wastes, are recognized as efficient biosorbents capable of removing pollutants from aqueous solutions. Compared to other removal techniques, biosorption offers several advantages, including low biosorbent cost, rapid process kinetics, high contaminant uptake under a wide range of pH and temperature conditions, the potential for biosorbent regeneration and reuse, and ease of storage (Azeez & Al-Zuhairi, 2022).

In this study, a synthetic dye solution was prepared by mixing equal amounts of three dyes: anionic Telon Blue AGLF (TB), cationic Astrazon Blue BG (AB), and nonionic Dianix Brilliant Blue R (DB). Three different adsorbents were simultaneously used at varying dosages to treat synthetic aqueous solutions containing fixed initial dye concentrations via the adsorption method. Magnolia cone (MC), the natural clay mineral beidellite (BD), and fly ash (FA) derived from a thermal power plant were selected as alternative adsorbents to commercial materials due to their abundance in nature, renewability, and low cost. While conventional adsorption-based wastewater treatment processes generally utilize a single type

of adsorbent, this study adopts a novel approach by employing three different adsorbents simultaneously. This strategy aims to enhance dye removal efficiency by exploiting the complementary adsorption capacities and surface characteristics of each material. In this study, the effects of various experimental parameters, including the simultaneous use of three different adsorbents, the individual dosages of each adsorbent (0.01–0.04 g), contact time (5–60 min), and pH (4–11), on the removal efficiencies of individual dyes and total organic carbon (TOC) were investigated. These independent variables were optimized for dye and TOC removal using the response surface methodology (RSM). Additionally, SEM and BET analyses were conducted to characterize the adsorbents before and after the adsorption process.

2 Materials and Methods

2.1 Preparation and Characterization of Adsorbents

MC used in the experimental studies was collected from the Kartepe district of Kocaeli. BD, a natural clay mineral, was obtained from clay deposits located in the Black Sea region, while FA was sourced from a thermal power plant.

MC was initially washed with tap water followed by distilled water to remove surface impurities and then dried at 85 °C for 48 h. After separating the flaky parts from the core, the material was ground into powder form. Subsequently, 30 g of MC was modified by stirring in 0.1 N NaOH solution at 200 rpm for 1 h. The modified MC was rinsed with ultrapure water until a neutral pH was achieved, then dried at 85 °C for 48 h to reach a constant weight.

BD and FA were used without any chemical pretreatment. They were dried at 105 °C for 24 h to eliminate moisture, and then crushed and ground into fine particles. All adsorbents were stored separately in moisture-free conditions.

The surface morphologies of MC, FA and BD were characterized using a Scanning Electron Microscope (SEM; Philips XL-30-SFEG, USA). Specific surface area measurements of the adsorbents were conducted via Brunauer–Emmett–Teller (BET) analysis using a MICROMERITICS/ASAP 2020 instrument (USA).

Batch adsorption experiments were carried out using this mixed dye solution. The effects of various operational parameters including adsorbent type (MC, BD, and FA), adsorbent dosage (0.01–0.04 g), contact time (5–60 min), and initial pH (4–11) on dye removal efficiency were systematically investigated. During each experiment, a known amount of adsorbent was added to 50 mL of dye solution in Erlenmeyer flasks and agitated at constant speed using a mechanical shaker.

After the specified contact time, the suspensions were filtered through a 0.45 µm membrane filter to remove solid residues. The concentrations of dyes in the filtrates was determined using high-performance liquid chromatography (HPLC). The analyses were performed with a Proshell 120 EC-C18 column (4.6×50 mm, 2.7 µm particle size) maintained at 25 °C. The mobile phase consisted of 40% acetonitrile (HPLC grade, Merck, Türkiye), 40% methanol, and 20% ultrapure water containing 82 g of cetyltrimethylammonium bromide (CTAB). (Salleh et al., 2011). The flow rate was set at 2 mL/min, and the detection wavelength (λ) was 597 nm. The mobile phase was degassed prior to use using an ultrasonic bath (Kudos SK2210HP model) to eliminate air bubbles and ensure analytical stability. The system operated under a pressure of approximately 60 bar during the measurements.

TOC analyses of the samples collected at the end of the test period were performed using a Shimadzu TOC-L analyzer at 680 °C, in accordance with the APHA 5310 B method (1998).

2.2 Preparation of Dye Solutions and Batch Adsorption Experiments

Anionic TB, cationic AB, and nonionic DB dyes were used as model pollutants in the study. Dyes were obtained from Dyestar, Tekirdağ, Türkiye. The physical and chemical characteristics of the dyes used in this study are summarized in Table 1 and Fig. 1.

Each dye was dissolved in ultrapure water to prepare stock solutions at a concentration of 1000 mg/L. From these stock solutions, equal volumes were mixed to obtain a synthetic dye solution containing 100 mg/L of each dye. The pH of the dye solutions was adjusted using 1 M NaOH or 1 M HCl to obtain the desired pH values prior to the experiments.

Samples containing different concentrations of each dye were analyzed using the HPLC system. Calibration curves for TB, AB, and DB were generated

Table 1 Molecular formula, molecular weight, λmax, and dye type

Dye	Molecular formula	Molecular weight (g/mol)	λmax	Type
TB, CAS Registery Number: 6378–87-6	$C_{37}H_{38}N_5NaO_6S_2$	735.85	610	Anionic dye
AB, CAS Registery Number: 33203–82-6	$C_{20}H_{26}ClN_3O$	359.89	654	Cationic dye
DB, CAS Registery Number: 12222–78-5	$C_{20}H_{14}N_2O_5$	362.34	624	Nonionic dye

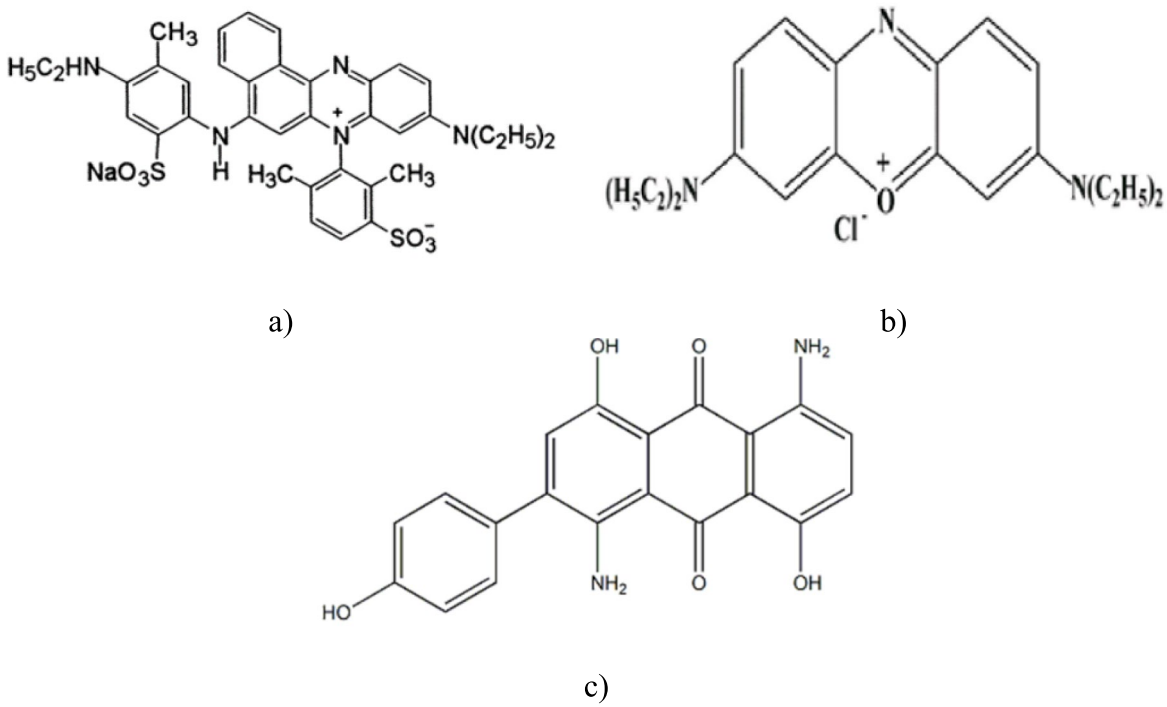


Fig. 1 The chemical structures of **a** TB, **b** AB, and **c** DB

by the system software based on the corresponding peak areas.

2.3 Experimental Design and Optimization

Traditional optimization methods, which examine responses by varying one factor at a time, are both time-consuming and costly, particularly in multi-variable systems, and they do not account for interactions between variables. In contrast, statistical experimental design techniques offer a more efficient approach for optimizing parameters in complex systems, allowing the consideration of variable interactions and the development of significant models with a minimal number of experiments. Within this context, the response surface methodology (RSM) is employed to investigate the relationship between independent variables and responses and can be applied using linear or non-linear models. The central composite design (CCD), commonly used in RSM, is particularly preferred for second-order model fitting, enabling the evaluation of variable effects and experimental errors with a limited number of trials (Baahmadi et al., 2025; Kus et al., 2025). In this study, the experimental design was constructed using the Central Composite Design (CCD) approach implemented in Design-Expert software (8.0.3 trial version, Stat-Ease Inc., Minneapolis, USA). A total of 50 experimental runs were generated to optimize the adsorption conditions and evaluate the effects of selected variables on dye

and TOC removal efficiencies. The input variables were adsorbent dose (g), contact time (min), and pH, while the response variables were dye removal (%) and TOC removal (%). To assess experimental reproducibility and model adequacy, eight replicates were conducted at the center point, corresponding to the following conditions: 0.03 g of each adsorbent (MC, BD, and FA), pH 7.5, and 32.5 min of contact time. These center point repetitions allowed for the estimation of experimental error and potential curvature in the response surface. The experimental variables are presented in Table 2.

3 Results and Discussion

3.1 Characterization of Adsorbents

Figures 2a, 2c and 2e show SEM images of the adsorbents before adsorption. Examination of these images revealed that all samples exhibited rough, lamellar, porous and heterogeneous morphologies prior to adsorption. These morphological characteristics suggest that the adsorbents have a favourable surface structure for physical adsorption. Furthermore, a porous structure is considered an important feature for adsorption efficiency as it reduces mass transfer resistance within the adsorbent (Zeng et al., 2024).

SEM analysis revealed clear morphological changes in the adsorbents after the adsorption process (Fig. 2b, Fig. 2d and Fig. 2f). As can be seen in Fig. 2a, the surface of the MC appeared irregular, porous and rough before adsorption. After adsorption, however, it became smoother with partially filled pore openings (Fig. 2b). This observation suggests that the surface of MC was covered by dye molecules, leading to partial pore blockage and a reduction in available active sites. In the case of FA, the pre-adsorption surface showed an amorphous and fragmented structure, with loosely bound particles and visible voids (Fig. 2c). After adsorption, the surface became more compact, although some micropores remained open (Fig. 2d). This indicates that FA underwent limited surface interaction, implying a lower number of active sites participating in dye binding. BD, on the other hand, initially exhibited a distinct layered morphology (Fig. 2e). Following adsorption (Fig. 2f), the layers appeared more compact and covered, with most of the pores filled. This suggests that strong adsorption occurred both on the surface and within the interlayer spaces of BD.

As seen from the Table 3, BET surface area analysis supported these morphological findings, showing a clear decrease in surface area after adsorption for all adsorbents. For MC, the SBET value dropped from 158.50 to 90.16 m^2/g, indicating that dye molecules occupied a considerable portion of the active sites and internal pores. FA exhibited the smallest change, with its surface area decreasing from 113.37 to 100.99 m^2/g, confirming its relatively limited adsorption capacity. In contrast, BD showed the most significant reduction, from 157.51 to 18.99 m^2/g, suggesting extensive pore filling and strong dye retention within its layered structure.

Overall, SEM and BET results consistently demonstrate that adsorption led to surface coverage and partial or complete pore blockage, resulting in a decline in available surface area. Among the three materials, BD showed the highest adsorption efficiency, followed by MC and then FA. These findings highlight that the adsorption mechanism primarily involves surface coverage and pore filling, and that the structural characteristics of each adsorbent play a key role in determining their adsorption performance (Lu et al., 2022).

Table 2 Independent variables and levels of the process

Factor	Name	Units	Low Actual	High Actual	Mean
A	FA	g/L	0.2	0.8	0.5
B	MC	g/L	0.2	0.8	0.5
C	BD	g/L	0.2	0.8	0.5
D	pH		4	11	7.5
E	Time	min	5	60	32.5

3.2 Design of Experiment and Statistical Analysis

Response Surface Methodology (RSM) is a statistical and mathematical approach employed to optimize the response of a system influenced by multiple independent variables. In this methodology, independent variables are treated as factors, while dependent variables are defined as responses. RSM is particularly effective for the modeling, analysis, and optimization of complex processes where the response is governed by the interactive effects of several variables (Igberase & Mkhize, 2025). Among the experimental

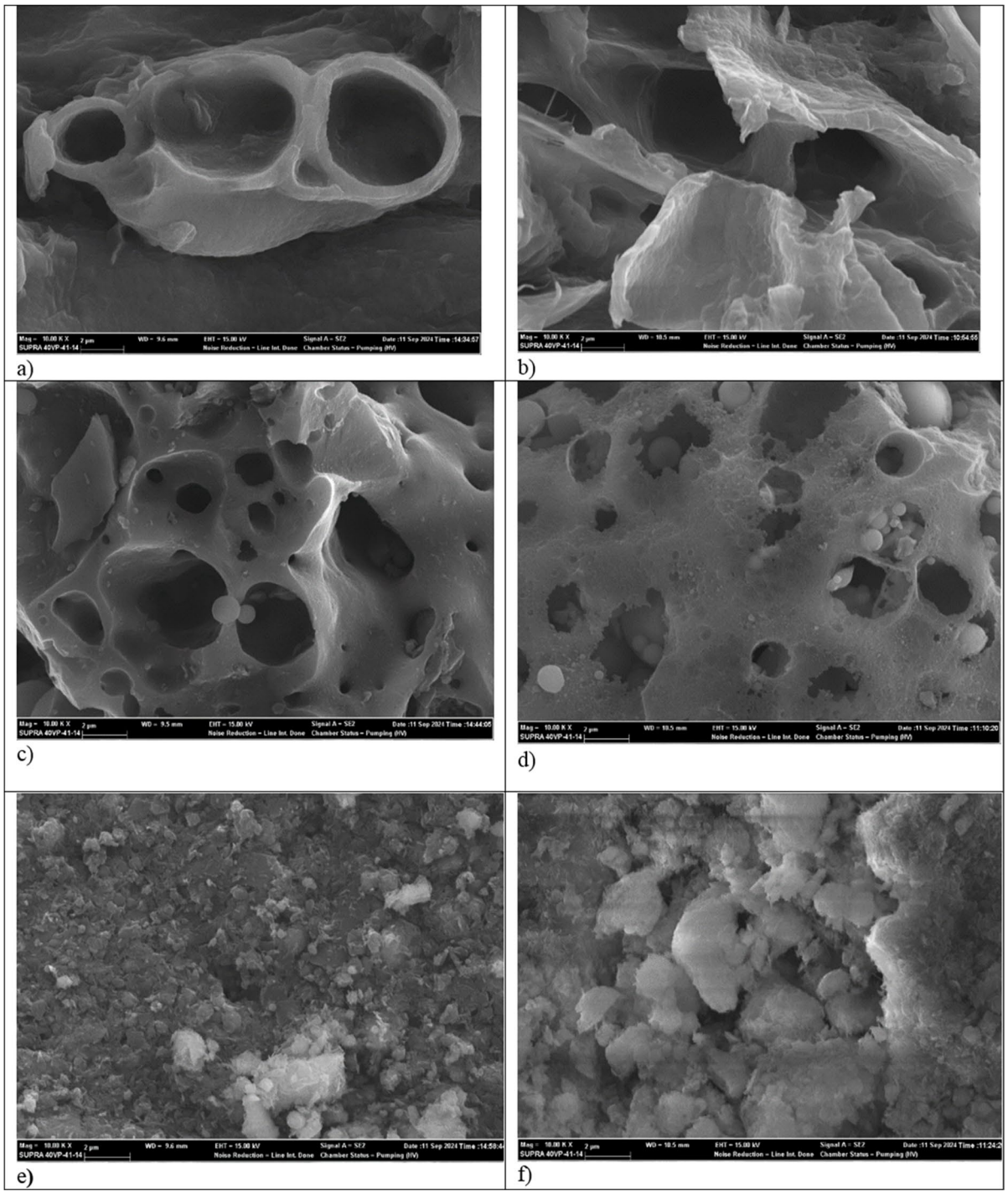


Fig. 2 SEM images of MC before **a** and after adsorption **b**; FA before **c** and after adsorption **d**; and BD before **e** and after adsorption **f**

Table 3 Results of BET analysis of before adsorption and after adsorption

Adsorbent	SBET (m^2/g) Before adsorption	SBET (m^2/g) After adsorption
MC	158.50	90.16
FA	113.37	100.99
BD	157.51	18.99

designs utilized within the scope of Response Surface Methodology (RSM), the Central Composite Design (CCD) is the most widely applied due to its high efficiency and adaptability. It enables comprehensive evaluation of individual variable effects and estimation of experimental error with a relatively low number of experimental runs (Baahmadi et al., 2025).

The experimental design consisted of 50 experiments with five factors, three levels and eight replication experiments. Equation (1) was used to determine the total number of experimental runs (N).

$$N = K^2 + 2K + C_P \quad (1)$$

where N is the number of experiments, K is the number of parameters and C_p is the number of repeat experiments.

The experimental factors of this study and their effect on the removal efficiency of AB, DB, TB and TOC are given in Table 4.

A design consisting of a total of 50 experiments was created with the Design Expert software (8.0.3). Experimental studies were repeated 8 times under the conditions of 0.03 g each of MC, BD and FA of the center point, pH 7.5 and 32.5 min experimental time. Table 5 gives the model statistics of the proposed adsorption test for dyestuff and TOC removal. The model adequacy was evaluated by comparing the coefficient of determination (R^2) values for linear, two-factor interaction (2FI), quadratic, and cubic models. As shown in Table 5, the R^2 values for the quadratic models were 0.79, 0.76, 0.80, and 0.84 for AB, DB, TB, and TOC responses, respectively. These values are significantly higher than those of the linear and 2FI models, indicating that the quadratic terms provide a better fit for describing the nonlinear relationship between the process variables and the responses. Although the cubic models yielded higher R^2 values (0.91–0.96), they were aliased, suggesting over parameterization and potential model instability. Therefore, the quadratic model was selected as the most appropriate for predicting the adsorption behavior of the dye mixture and total organic carbon (TOC) removal. The R^2 values above 0.75 demonstrate that the developed models adequately represent the experimental data and can be reliably used for process optimization purposes. Similar findings have been reported in previous studies employing response surface methodology for multicomponent dye adsorption systems, where quadratic models provided the most statistically significant fits compared to linear or 2FI models (Asaad et al., 2025). The quadratic model was selected as the most appropriate model considering the R^2 values.

The equations (Eqs. 2–5) for AB, DB, TB and TOC removal with the help of quadratic model are given below.

$$\begin{aligned} AB = {} & +78.06 - 0.096 * A - 0.32 * B + 3.48 * C \\ & + 3.78 * D + 1.66 * E + 3.35 * A * B - 2.90 * A * C \\ & + 2.21 * C * D - 2.63 * C * E - 3.16 * C^2 \end{aligned} \quad (2)$$

$$\begin{aligned} DB = {} & +81.57 - 0.22 * A - 3.03 * B + 1.32 * C \\ & + 7.06 * D + 3.10 * E + 3.45 * A * B \\ & - 3.45 * D * E - 4.02 * D^2 \end{aligned} \quad (3)$$

$$\begin{aligned} TB = {} & +34.71 - 1.22 * A - 0.76 * B - 1.21 * C + 0.74 * D \\ & + 6.33 * E + 5.44 * B * D - 3.18 * C * E \\ & + 4.12 * D * E + 4.12A^2 + 4.57B^2 + 3.62C^2 + 2.22D^2 \end{aligned} \quad (4)$$

$$\begin{aligned} TOC = {} & +45.49 - 1.31 * A + 1.73 * B + 2.15 * C + 1.25 * D \\ & + 2.11 * E + 1.62 * A * B - 1.58 * A * C - 1.79 * B * C \\ & + 2.10 * B * E + 2.71 * D * E - 2.55 * C^2 + 2.50 * D^2 \end{aligned} \quad (5)$$

where A (g/L) is the amount of FA, B (g/L) is the amount of MC, C (g/L) is the amount of BD, D is pH, E (min) is the duration of the experiment. Considering the correlation coefficient (R^2) which indicates the validity and significance of the model for all three dyes and TOC removal, "Quadratic Model" was selected. ANOVA analysis according to the quadratic model for AB, DB, TB and TOC are shown in Tables 6, 7, 8 and 9.

As shown in Table 6, the ANOVA results for AB indicate that the model is statistically significant, as evidenced by the Model F-value of 11.46. The

Table 4 Center composite design test table and test results

	A	B	C	D	E	AB Removal (%)		DB Removal (%)		TB Removal (%)		TOC Removal (%)	
Run	FA (g/L)	MC (g/L)	BD (g/L)	pH	Time (min)	Actual Value	Predic. Value	Actual Value	Predic. Value	Actual Value	Predic Value	Actual Value	Predic. Value
1	0.03	0.03	0.03	4.00	32.50	64.94	69.07	38.63	42.01	39.38	45.50	26.25	28.36
2	0.02	0.03	0.02	6.03	20.94	53.3	59.08	41.50	56.34	36.20	39.33	35.72	37.18
3	0.03	0.03	0.03	7.50	60.00	81.55	82.02	81.74	88.95	50.27	49.77	48.31	50.50
4	0.02	0.03	0.03	8.97	20.94	84.44	84.67	87.63	80.02	47.92	47.41	40.31	38.13
5	0.02	0.02	0.02	6.03	20.94	70.73	66.42	74.37	69.30	66.63	5172	41.69	37.57
6	0.03	0.03	0.03	6.03	20.94	72.90	73.40	71.90	65.44	30.70	40.84	40.49	38.51
7	0.02	0.02	0.03	8.97	20.94	83.30	92.01	88.80	92.98	31.00	38.04	45.54	45.70
8	0.03	0.03	0.02	8.97	20.94	71.50	74.53	83.70	83.83	36.00	41.03	43.27	38.03
9	0.03	0.03	0.03	8.97	44.06	79.01	83.44	84.64	85.78	58.60	59.50	47.94	49.42
10	0.03	0.02	0.03	8.97	20.94	74.70	79.31	88.55	85.66	46.03	35.61	35.71	36.67
11	0.02	0.03	0.02	8.97	20.94	58.72	62.22	79.27	77.37	43.32	43.46	31.46	34.27
12	0.03	0.03	0.03	11.0	32.50	90.07	87.05	79.23	75.62	58.63	49.04	36.83	34.31
13	0.01	0.03	0.03	7.50	32.50	80.91	78.29	93.44	82.08	62.99	60.92	47.35	48.61
14	0.03	0.03	0.01	7.50	32.50	53.44	51.90	86.63	78.42	59.50	58.07	21.16	25.96
15	0.03	0.03	0.03	7.50	32.50	81.00	78.06	73.85	81.57	38.33	34.71	45.31	45.49
16	0.03	0.02	0.03	8.97	44.06	75.79	77.38	84.66	84.96	50.88	50.14	44.69	42.11
17	0.02	0.02	0.03	8.97	44.06	88.95	90.08	92.58	92.28	57.85	52.57	46.99	51.14
18	0.02	0.03	0.03	6.03	44.06	76.69	70.75	83.86	72.10	43.30	41.34	45.14	44.04
19	0.03	0.01	0.03	7.50	32.50	78.14	78.82	94.59	88.78	58.45	62.35	45.85	41.37
20	0.04	0.03	0.03	7.50	32.50	78.65	77.83	83.12	81.06	56.52	55.12	44.21	42.36
21	0.02	0.02	0.02	8.97	44.06	74.15	78.15	80.27	89.63	58.39	61.35	43.90	40.09
22	0.03	0.02	0.02	8.97	44.06	75.73	77.06	82.26	82.31	57.07	58.92	33.97	37.37
23	0.03	0.03	0.03	6.03	44.06	66.01	74.46	83.61	78.56	38.79	38.90	38.92	41.51
24	0.03	0.03	0.03	7.50	32.50	71.00	78.06	79.62	81.57	37.00	34.71	44.66	45.49
25	0.03	0.03	0.03	7.50	32.50	81.00	78.06	82.00	81.57	36.00	34.71	43.62	45.49
26	0.03	0.02	0.03	6.03	20.94	76.00	67.33	55.10	64.62	47.80	83.23	36.26	39.59
27	0.03	0.02	0.02	6.03	20.94	57.01	65.33	57.01	61.98	41.52	49.29	31.20	34.85
28	0.02	0.03	0.02	8.97	44.06	66.24	70.81	79.55	76.67	51.11	70.72	49.57	48.10
29	0.02	0.02	0.02	8.97	20.94	74.78	69.56	84.33	90.33	23.20	34.09	32.29	34.65
30	0.03	0.03	0.03	7.50	32.50	82.23	78.06	89.53	81.57	35.80	34.71	48.83	45.49
31	0.03	0.03	0.03	7.50	32.50	82.26	78.06	84.10	81.57	36.80	34.71	43.05	45.49
32	0.03	0.03	0.03	7.50	32.50	82.95	78.06	80.59	81.57	27.00	34.71	42.45	45.49

Table 4 (continued)

	A	B	C	D	E	AB Removal (%)		DB Removal (%)		TB Removal (%)		TOC Removal (%)	
Run	FA (g/L)	MC (g/L)	BD (g/L)	pH	Time (min)	Actual Value	Predic. Value	Actual Value	Predic. Value	Actual Value	Predic Value	Actual Value	Predic. Value
33	0.03	0.03	0.03	7.50	32.50	83.61	78.06	82.66	81.57	27.85	34.71	45.96	45.49
34	0.02	0.03	0.03	6.03	20.94	64.74	72.69	59.23	58.98	42.18	43.28	41.36	41.05
35	0.03	0.03	0.03	7.50	5.00	75.43	74.11	74.58	74.19	37.22	19.65	42.49	40.47
36	0.03	0.03	0.02	8.97	44.06	80.77	83.12	83.29	83.13	80.42	68.29	50.51	51.86
37	0.03	0.04	0.03	7.50	32.50	83.91	77.30	55.52	74.35	66.12	58.75	48.80	49.61
38	0.03	0.03	0.02	6.03	20.94	72.10	71.39	79.10	62.80	35.50	36.89	42.16	40.95
39	0.03	0.02	0.02	8.97	20.94	70.2	68.47	78.30	83.01	30.40	31.66	31.56	37.93
40	0.03	0.03	0.02	6.03	44.06	82.53	79.98	75.45	75.91	56.90	47.68	48.25	43.95
41	0.03	0.03	0.03	8.97	20.94	84.7	85.38	80.10	86.48	34.00	44.97	29.01	35.59
42	0.02	0.02	0.03	6.03	44.06	71.31	78.10	79.88	85.05	54.06	53.74	37.07	43.22
43	0.02	0.02	0.03	6.03	20.94	80.7	80.03	72.50	71.94	64.00	55.67	49.10	48.61
44	0.02	0.03	0.02	6.03	44.06	63.56	67.67	61.14	69.45	52.53	50.12	42.10	40.18
45	0.03	0.02	0.02	6.03	44.06	77.44	73.91	85.12	75.09	68.85	60.08	31.01	29.45
46	0.03	0.03	0.04	7.50	32.50	73.94	68.46	81.50	84.71	54.37	52.32	41.40	36.20
47	0.02	0.02	0.02	6.03	44.06	78.77	75.01	80.69	82.41	60.00	62.52	34.71	32.17
48	0.03	0.02	0.03	6.03	44.06	62.8	65.40	74.91	77.73	45.81	51.30	36.21	34.19
49	0.03	0.03	0.03	7.50	32.50	84.04	78.06	82.68	81.57	26.58	37.71	47.41	45.49
50	0.02	0.03	0.03	8.97	44.06	87.59	82.73	86.87	79.32	65.50	61.94	53.67	51.96

Table 5 Model statistics of adsorption test for dyestuff and TOC removal

Source of Variation	R^2			
	Linear	Two-factor interaction	Quadratic	Cubic
AB	0.33	0.61	0.79 (proposed)	0.91 (Aliased)
DB	0.43	0.58	0.76 (proposed)	0.94 (Aliased)
TB	0.22	0.50	0.80 (proposed)	0.91 (Aliased)
TOC	0.27	0.55	0.84 (proposed)	0.95 (Aliased)

probability that such a large F-value could occur due to random noise is only 0.01%, confirming the significance of the model. A *P*-value less than 0.0500 indicates the statistical significance of the associated model terms. In this context, the terms C, D, E, AB, AC, CD, CE, and C^2 were found to be significant contributors to the model. Conversely, terms with *P*-values greater than 0.1000 are considered statistically insignificant under the investigated conditions. Furthermore, the Lack of Fit F-value of 1.51 implies that the lack of fit is not statistically significant relative to the pure error, with a 29.71% probability that such a value could arise from noise, indicating that the model adequately represents the experimental data within the studied parameter range.

According to the ANOVA results for DB adsorption presented in Table 7, the Model F-value of 11.13

Table 6 The quadratic model's ANOVA result for AB adsorption

Source	Sum of Squares	Df	Mean Square	F- value	p—value
Model	2860.03	10	286.00	11.46	< 0.0001 significant
A-FA	0.40	1	0.40	0.016	0.9001
B-MC	4.42	1	4.42	0.18	0.6762
C-BD	525.42	1	525.42	21.05	< 0.0001
D-pH	619.06	1	619.06	24.80	< 0.0001
E-Time	119.94	1	119.94	4.81	0.0344
AB	359.52	1	359.52	14.40	0.0005
AC	269.35	1	269.35	10.79	0.0022
CD	156.11	1	156.11	6.25	0.0167
CE	221.45	1	221.45	8.87	0.0050
C^2	584.36	1	584.36	23.41	< 0.0001
Lack of Fit	850.51	32	26.58	1.51	0.2971 not significant
Error	383349	49			

Table 7 The quadratic model's ANOVA result for DB adsorption

Source	Sum of Squares	Df	Mean Square	F- value	p—value
Model	4762.80	8	595.35	11.13	< 0.0001 significant
A-FA	2.00	1	2.00	0.037	0.8475
B-MC	398.71	1	398.71	7.45	0.0093
C-BD	75.72	1	75.72	1.41	0.2411
D-pH	216172	1	2161.72	40.40	< 0.0001
E-Time	417.16	1	417.16	7.80	0.0079
AB	379.85	1	379.85	7.10	0.0110
DE	381.64	1	381.64	7.13	0.0108
D^2	946.00	1	946.00	17.68	0.0001
Lack of Fit	2058.04	34	60.53	3.12	0.0607 not significant
Error	135.97	7	19.42		

Table 8 The quadratic model's ANOVA result for TB adsorption

Source	Sum of Squares	Df	Mean Square	F- value	p—value
Model	6136.98	12	511.41	7.78	< 0.0001 significant
A-FA	64.38	1	64.38	0.98	0.3286
B-MC	24.80	1	24.80	0.38	0.5427
C-BD	63.20	1	63.20	0.96	0.3331
D-pH	23.94	1	23.94	0.36	0.5497
E-Time	1735.82	1	1735.82	26.42	< 0.0001
BD	947.43	1	947.43	14.42	0.0005
CE	324.11	1	324.11	4.93	0.0326
DE	542.36	1	542.36	8.28	0.0067
A^2	960.03	1	960.03	14.61	0.0005
B^2	1179.76	1	1179.76	17.96	0.0001
C^2	741.77	1	741.77	11.29	0.0018
D^2	278.68	1	278.68	4.24	0.0465
Lack of Fit	2251.81	30	75.06	2.93	0.0716 not significant
Error	179.20	7	25.60		

Table 9 The quadratic model's ANOVA result for TOC

Source	Sum of Squares	Df	Mean Square	F- value	p—value
Model	1982.73	12	165.23	14.94	< 0.0001 significant
A-FA	74.82	1	74.82	6.77	0.0133
B-MC	129.85	1	129.85	11.74	0.0015
C-BD	200.45	1	200.45	18.12	0.0001
D-pH	67.73	1	67.73	6.12	0.018019271
E-Time	192.71	1	192.71	17.42	0.0002
AB	84.18	1	84.18	7.61	0.0090
AC	79.51	1	79.51	7.19	0.0109
BC	103.10	1	103.10	9.32	0.0042
BE	140.78	1	140.78	12.73	0.0010
DE	234.69	1	234.69	21.22	< 0.0001
C^2	376.03	1	376.03	34.00	< 0.0001
D^2	362.58	1	362.58	32.78	< 0.0001
Lack of Fit	375.60	30	12.52	2.61	0.0953 not significant
Error	33.61	7	4.80		

indicates that the model is statistically significant. The probability that such a high F-value could occur due to random noise is only 0.01%, demonstrating the model's reliability. A *P*-value less than 0.0500 suggests that the corresponding model terms are statistically significant. In this case, the terms B, D, E, AB, DE, and D^2 are identified as significant contributors. Conversely, terms with *P*-values greater than 0.1000 are considered statistically insignificant. The Lack of Fit F-value is 3.12, indicating that there is a 6.07% probability that this magnitude of lack of fit could be attributed to random variation, suggesting that the lack of fit is not statistically significant and that the model adequately represents the experimental data within the studied parameter range.

As presented in Table 8, the ANOVA results for TB adsorption demonstrate that the quadratic model is statistically significant, as indicated by a Model F-value of 7.78 ($p < 0.0001$). Based on the ANOVA analysis, the linear term E (contact time), the interaction terms BD, CE, and DE, as well as the quadratic terms A^2, B^2, C^2, and D^2 were identified as

statistically significant contributors to TB removal, whereas the remaining terms exhibited negligible effects under the investigated conditions. The prominence of quadratic terms suggests a non-linear response of TB adsorption to the studied variables. The Lack of Fit F-value of 2.93 corresponds to a p-value of 0.0716, indicating that the lack of fit is not statistically significant and that the model adequately represents the experimental data within the studied parameter range.

As shown in Table 9, the ANOVA results for TOC removal indicate that the quadratic model is statistically significant, with a Model F-value of 14.94 ($p < 0.0001$). The linear terms A, B, C, D, and E, the interaction terms AB, AC, BC, BE, and DE, as well as the quadratic terms C^2 and D^2 were identified as statistically significant contributors to TOC removal, whereas the remaining terms exhibited negligible effects under the investigated conditions. The presence of multiple significant linear, interaction, and quadratic terms indicates that TOC removal is governed by the combined and non-linear effects of the operational parameters rather than by a single dominant factor. The significance of interaction terms suggests that the influence of one parameter depends on the level of others, while the quadratic terms reflect the existence of optimal operating ranges instead of a simple linear response. The Lack of Fit F-value of 2.61 corresponds to a p-value of 0.0953, indicating that the lack of fit is not statistically significant and that the model adequately represents the experimental data within the studied experimental domain.

Considering the overall findings, the ANOVA results demonstrated that the adsorption behaviours of individual dyes and TOC responded differently to the operational parameters, indicating distinct removal mechanisms. While the quadratic models developed for AB, DB, and TB adsorption were governed by a limited number of statistically significant factors and interactions, TOC removal exhibited a considerably more complex response pattern. The presence of multiple significant linear, interaction, and quadratic terms in the TOC model suggests that organic carbon removal is controlled by the simultaneous and interdependent effects of several parameters, rather than by a single dominant variable. This complexity reflects the heterogeneous nature of organic matter and the involvement of multiple adsorption pathways (Adewoye et al., 2021).

The significance of interaction and quadratic terms in the TOC model further indicates the existence of non-linear relationships and optimal operating ranges for the process variables. In particular, the observed quadratic effects imply that increasing certain parameters beyond specific thresholds does not necessarily enhance TOC removal and may even reduce efficiency due to surface saturation, competitive adsorption, or mass transfer limitations. Such behavior highlights the limitations of linear optimization approaches and underlines the importance of response surface methodology in capturing the true system dynamics. The interaction effects also suggest that variations in one operational parameter can alter the influence of others, emphasizing the coupled nature of the adsorption process in multi-parameter systems (Alkhaldi et al., 2024; Zhao et al., 2023).

Moreover, the discrepancy between the relatively high removal efficiencies observed for individual dyes and the more complex behaviour of TOC removal highlights the fundamental distinction between decolourization and overall organic carbon reduction. While dye adsorption effectively reduces color, it does not necessarily correspond to the complete removal of organic constituents. Therefore, the TOC results provide a more comprehensive assessment of treatment performance, indicating that colour removal alone may overestimate overall purification efficiency. These findings emphasize the need for multi-response evaluation when assessing adsorption-based treatment processes and suggest that optimization strategies should consider both target pollutant removal and broader organic load reduction (Hsu et al., 2024).

On the other hand, despite the robust experimental design and the statistically significant models obtained in this study, several limitations should be acknowledged. Firstly, the adsorption experiments were conducted under controlled batch conditions, which may not accurately reflect the complexity of real wastewater systems. In practical applications, the presence of additional organic and inorganic constituents, fluctuating pollutant concentrations and hydraulic variations could influence adsorption performance and alter the relative importance of operational parameters.

Secondly, while the central composite design allowed for the evaluation of linear, interaction and quadratic effects, the model predictions are only valid within the experimental ranges studied. Extrapolation

beyond these ranges may not accurately reflect system behaviour due to potential changes in adsorption mechanisms, surface saturation or mass transfer limitations. Therefore, the proposed models should be interpreted as optimisation tools within the defined parameter space, rather than as universally applicable predictive equations.

Additionally, the coefficient of determination (R^2) values obtained for some responses may be considered moderate compared to single-response or single-adsorbent systems. However, this outcome is largely attributable to the inherently multi-variable and multi-response nature of the studied system, which involves three different adsorbents, multiple operational parameters, and heterogeneous adsorption mechanisms. In such complex systems, a portion of the response variability may arise from non-modelled physicochemical interactions and experimental uncertainty, which cannot be fully captured by empirical models. Nevertheless, the statistical significance of the proposed quadratic models and the non-significant lack of fit indicate that the models are adequate for identifying key factors, interaction effects, and optimal operating trends within the investigated experimental domain.

Furthermore, although TOC removal was employed as an indicator of the reduction of organic matter, it does not offer insights into the specific composition or biodegradability of the residual organic fraction. High TOC removal does not necessarily imply complete mineralisation or reduced environmental risk. Future studies could benefit from complementary analyses, such as characterising the organic fraction or assessing toxicity, as well as validating the proposed adsorption system under continuous-flow or pilot-scale conditions to better assess its applicability.

Figure 3 presents the comparison between the predicted values obtained from the developed quadratic models and the experimentally measured data for (a) AB, (b) DB, (c) TB, and (d) TOC removal. Overall, the data points are distributed close to the diagonal reference line, indicating a reasonable agreement between model predictions and experimental observations. Among the studied responses, DB (Fig. 3b) exhibits a stronger correlation, suggesting that the model represents this response more consistently within the investigated range. Minor deviations are observed for TB (Fig. 3c), particularly at lower response values, which may be attributed to the increased variability associated with this adsorption process. For TOC removal (Fig. 3d), despite the relatively narrow response range, the predicted values follow the experimental trend, supporting the adequacy of the model in capturing the overall system behavior within the design space. These results indicate that the developed models are suitable for describing response trends and supporting process optimization under the studied experimental conditions.

4 Conclusion

The present study provides a novel and realistic approach to dye wastewater treatment by simultaneously evaluating the adsorption performance of three different adsorbents (MC, BD, and FA) for a mixed dye system containing anionic, cationic, and nonionic dyes. Unlike most previous studies that typically focus on a single adsorbent-single dye system under idealized laboratory conditions, this research represents industrial wastewater scenarios where multiple dyes coexist and interact. Central Composite Design (CCD) within the scope of Response Surface Methodology (RSM) was employed for optimization purposes conditions. Adsorbent dosage (0.01–0.04 g), pH (4–11), and contact time (5–60 min) were selected as independent variables, while dye and Total Organic Carbon (TOC) removal efficiencies were considered as response variables. Batch experiments were conducted under the conditions determined by RSM, and the resulting experimental data were analyzed to develop mathematical model equations capable of predicting dye and TOC removal efficiencies. The model results were compared with the experimental data, and the coefficients of determination (R^2) were found to be 0.79 for AB, 0.76 for BD, 0,80 for TB and 0.84 for TOC at a 95% confidence level. Furthermore, ANOVA analysis was performed to identify the significant process parameters and their two-way interactions. Finally, the optimum conditions for achieving maximum removal efficiencies were determined, and verification experiments were conducted under these optimized conditions. By combining different adsorbents in specific proportions, synergistic adsorption effects were achieved, leading to enhanced removal

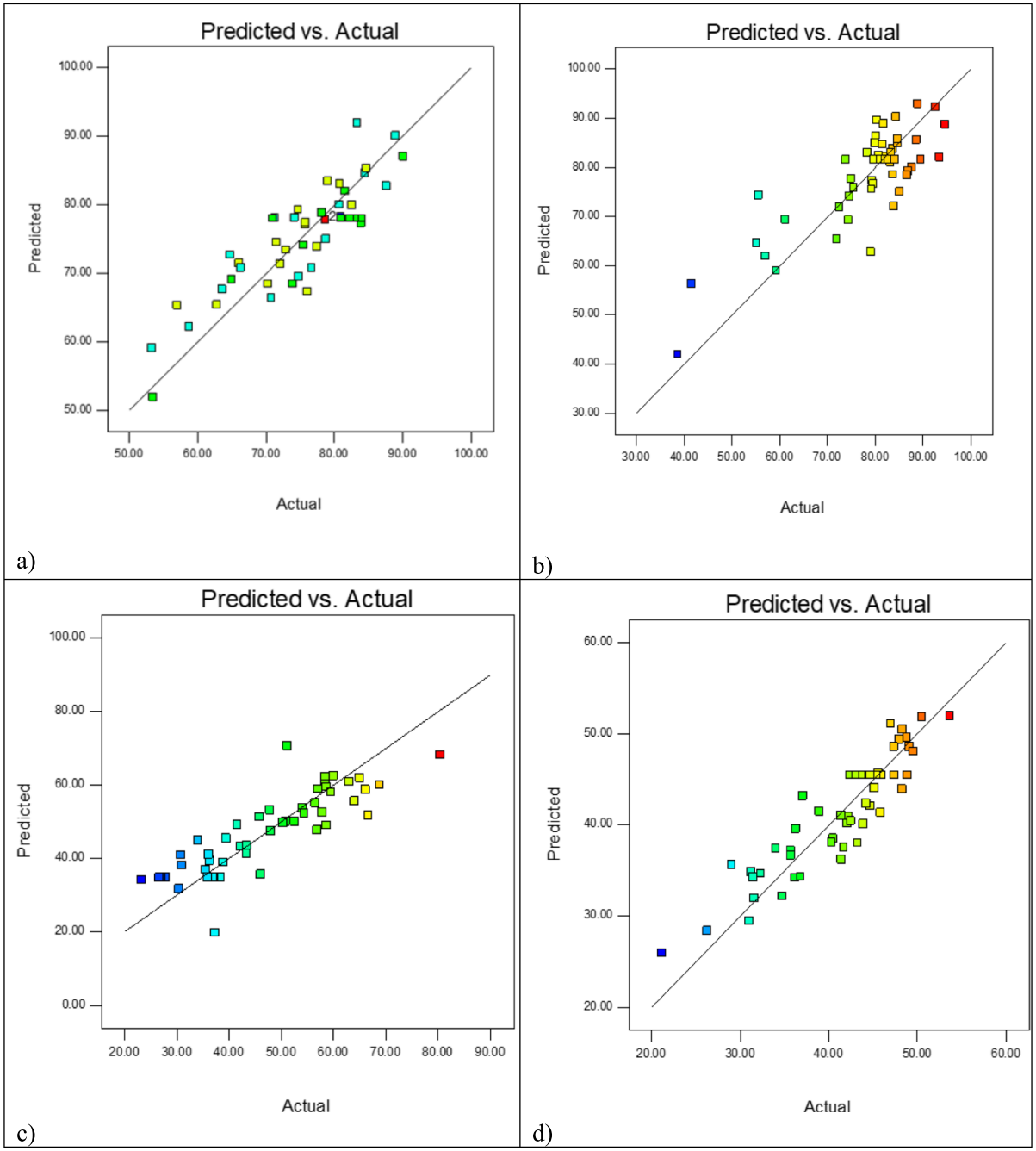


Fig. 3 Comparison of actual and experimental data (**a**: AB, **b**: DB, **c**: TB, **d**: TOC)

efficiencies and broader applicability across diverse dye types. In this study, statistically significant quadratic models were developed based on experimental data to describe the system behavior and support process optimization within the investigated parameter ranges.The sufficient agreement between the predicted and actual values demonstrates the reliability and accuracy of the proposed model. Among all parameters, DB exhibited the highest correlation, while minor deviations were observed

only at lower TB concentrations. Overall, the findings indicate that the developed models adequately describe the system behavior within the investigated parameter ranges and provide a useful framework for optimizing operational parameters. Overall, this work not only bridges the gap between laboratory-scale studies and real industrial challenges but also offers a practical framework for designing efficient adsorbent mixtures capable of handling complex multicomponent dye effluents.

Authors Contribution Sevgi Fersiz &Melike Isgoren: Conceptualization, Data Analysis, Visualization, Writing—original draft, Writing – review & editing, Erhan Gengec:, Supervision, Writing – review & editing, Suna Demir: Data Analysis.

Funding Open access funding provided by the Scientific and Technological Research Council of Türkiye (TÜBİTAK). This work has been supported by Tubitak 2209-A University Student Research Projects Support Program project undergrant number 1919B012302703.

Data Availability All data generated by this study are available from the corresponding author upon reasonable request.

Declarations

Ethics Approval All the authors listed have participated in this work and seen the manuscript.

Consent for Publication All the authors listed have participated in this work and seen the manuscript.

Competing Interests The authors declare no competing interests.

Open Access This article is licensed under a Creative Commons Attribution 4.0 International License, which permits use, sharing, adaptation, distribution and reproduction in any medium or format, as long as you give appropriate credit to the original author(s) and the source, provide a link to the Creative Commons licence, and indicate if changes were made. The images or other third party material in this article are included in the article's Creative Commons licence, unless indicated otherwise in a credit line to the material. If material is not included in the article's Creative Commons licence and your intended use is not permitted by statutory regulation or exceeds the permitted use, you will need to obtain permission directly from the copyright holder. To view a copy of this licence, visit http://creativecommons.org/licenses/by/4.0/.

References

Abdulhameed, A. S., Abdullah, S., Altamimi, A. A., Abualhaija, M., & Algburi, S. (2025a). Development of a schiff base-chitosan-vanillin/hydroxyapatite composite for effective brilliant green dye removal: Characterization, adsorption modeling, and cost analysis. *International Journal of Biological Macromolecules, 310*, Article 143140. https://doi.org/10.1016/j.ijbiomac.2025.143140

Abdulhameed, A. S., Abdullah, S., Al-Masud, A. A., Al Omari, R. H., Abualhaija, M., & Algburi, S. (2025b). Production of sustainable adsorbent of crosslinked chitosan-oxalate and modified mango (*Mangifera indica* L.) seed for highly efficient adsorption of crystal violet dye: Water treatment and biomass valorization. *Biomass and Bioenergy, 199*, Article 107889. https://doi.org/10.1016/j.biombioe.2025.107889

Adewoye, T. L., Ogunleye, O. O., Abdulkareem, A. S., Salawudeen, T. O., & Tijani, J. O. (2021). Optimization of the adsorption of total organic carbon from produced water using functionalized multi-walled carbon nanotubes. *Heliyon*. https://doi.org/10.1016/j.heliyon.2020.e05866.

Alkhaldi, H., Alharthi, S., Alharthi, S., AlGhamdi, H. A., AlZahrani, Y. M., Mahmoud, S. A., Amin, L. G., Al-Shaalan, N. H., Boraie, W. E., Attia, M. S., Al-Gahtany, S. A., Aldaleeli, N., Ghobashy, M. M., Sharshir, A. I., Madani, M., Darwesh, R., & Abaza, S. F. (2024). Sustainable polymeric adsorbents for adsorption-based water remediation and pathogen deactivation: A review. *RSC Advances, 14*(45), 33143–33190. https://doi.org/10.1039/d4ra05269b

Asaad, S. M., Inayat, A., Jamil, F., & Hellier, P. (2025). Process optimization of biodiesel production from waste cooking oil and Neem oil blend. *Energies, 18*(18), Article 4944. https://doi.org/10.3390/en18184944

Azeez, R. A., & Al-Zuhairi, F. K. I. (2022). Biosorption of dye by immobilized yeast cells on the surface of magnetic nanoparticles. *Alexandria Engineering Journal, 61*(7), 5213–5222. https://doi.org/10.1016/j.aej.2021.10.044

Baahmadi, F., Abbasi-Asl, H., Ghaedi, M., Sabzehmeidani, M. M., & Shokrollahi, A. (2025). High-performance cellulose acetate fibers-loaded Alca layered double oxide adsorbents towards efficient elimination of anionic pollutants: Mechanism adsorption and RSM-CCD approach. *International Journal of Biological Macromolecules, 284*, Article 137788. https://doi.org/10.1016/j.ijbiomac.2024.137788

Daneshvar, E., Vazirzadeh, A., Niazi, A., Kousha, M., Naushad, M., & Bhatnagar, A. (2017). Desorption of methylene blue dye from brown macroalga: Effects of operating parameters, isotherm study and kinetic modeling. *Journal of Cleaner Production, 152*, 443–453. https://doi.org/10.1016/j.jclepro.2017.03.119

Gengec, N. A., Isgoren, M., Kobya, M., Veli, S., & Gengec, E. (2018). Optimization of beidellite/polyaniline production conditions by central composite design for removal of acid yellow 194. *Journal of Polymers and the Environment, 26*(6), 2619–2631. https://doi.org/10.1007/s10924-017-1157-4

Hsu, C. Y., Ali, E., Al-Saedi, H. F. S., Mohammed, A. Q., Mustafa, N. K., Talib, M. B., Radi, U. K., Ramadan, M. F., Ami, A. A., Al-Shuwaili, S. J., Alawadi, A., Alsalamy, A., & Baharinikoo, L. (2024). A chemometric approach based on response surface methodology for optimization of antibiotic and organic dyes removal from water samples. *BMC Chemistry, 18*(1), Article 5. https://doi.org/10.1186/s13065-023-01107-w

Igberase, E., & Mkhize, I. G. (2025). Efficient adsorption of methylene blue (MB) by an eco-friendly chitosan derivative adsorbent: An RSM and ANN modeling study. *Desalination and Water Treatment, 321*, Article 100943. https://doi.org/10.1016/j.dwt.2024.100943

Isgoren, M. (2024). Kinetics and thermodynamics of Isolan Bordeaux 2S-B dye adsorption on chemically synthesized graphene particles. *Fullerenes, Nanotubes and Carbon Nanostructures, 32*(7), 664–675. https://doi.org/10.1080/1536383X.2024.2320148

Isgoren, M., Fersiz, S., & Gengec, E. (2025). A novel, simply prepared biosorbent for the removal of cationic dye: characterization, isotherm, kinetic and thermodynamic study. *Journal of Dispersion Science and Technology*, 1–17. https://doi.org/10.1080/01932691.2025.2558143

Jha, S., Gaur, R., Shahabuddin, S., Tyagi, I., Giri, J., & Kanan, M. (2025). Utilizing low-cost mausambi peel-derived adsorbents for the effective treatment of complex industrial dye mixture in wastewater: Unravelling the adsorption mechanism. *Cleaner Engineering and Technology, 26*, Article 100951. https://doi.org/10.1016/j.clet.2025.100951

Khan, M. D., Singh, A., Khan, M. Z., Tabraiz, S., & Sheikh, J. (2023). Current perspectives, recent advancements, and efficiencies of various dye-containing wastewater treatment technologies. *Journal of Water Process Engineering, 53*, Article 103579. https://doi.org/10.1016/j.jwpe.2023.103579

Kus, B., Sezer, M., Isgoren, M., & Veli, S. (2025). Anodic electrooxidation of textile wastewater by using spray coating Ti/TiO2–RuO2–IrO2 anode: Response surface optimization of the process. *Journal of the Indian Chemical Society, 102*, Article 101595. https://doi.org/10.1016/j.jics.2025.101595

Lu, Y., Liu, Y., Li, C., Liu, H., Liu, H., Tang, Y., & Wang, C. (2022). Adsorption characteristics and mechanism of methylene blue in water by NaOH-modified areca residue biochar. *Processes, 10*(12), Article 2729. https://doi.org/10.3390/pr10122729

Mokhtar, N., Aziz, E. A., Aris, A., Shukor, H., & Zaki, S. M. (2024). Biosorption of anionic and cationic azo dye onto red macro alga: Determination of the significant variables using resolution V fractional factorial design. *Physics and Chemistry of the Earth, Parts a, b, and C, 134*, Article 103593. https://doi.org/10.1016/j.pce.2024.103593

Nath, J., Dewan, M., Ghosh, A., Ray, S. S., Orasugh, J. T., Lahiri, B., & Adhikari, A. (2025). Chitosan-based adsorbents for remediation of toxic dyes from wastewater: A review on adsorption mechanism, reusability, machine learning based modeling and future perspectives. *International Journal of Biological Macromolecules*. https://doi.org/10.1016/j.ijbiomac.2025.143388

Salleh, M. A. M., Mahmoud, D. K., Karim, W. A. W. A., & Idris, A. (2011). Cationic and anionic dye adsorption by agricultural solid wastes: A comprehensive review. *Desalination, 280*(1–3), 1–13. https://doi.org/10.1016/j.desal.2011.07.019

Shao, S., Xu, Z., Xia, S., & Gao, G. (2025). Mechanistic and adsorption kinetics study of sulfonated activated carbon enhanced starch-based aerogel for high efficient adsorption of cationic and anionic dyes. *International Journal of Biological Macromolecules, 309*, Article 142555. https://doi.org/10.1016/j.ijbiomac.2025.142555

Shi, Y., Chang, Q., Zhang, T., Song, G., Sun, Y., & Ding, G. (2022). A review on selective dye adsorption by different mechanisms. *Journal of Environmental Chemical Engineering, 10*(6), Article 108639. https://doi.org/10.1016/j.jece.2022.108639

Solayman, H. M., Hossen, M. A., Abd Aziz, A., Yahya, N. Y., Leong, K. H., Sim, L. C., & Zoh, K. D. (2023). Performance evaluation of dye wastewater treatment technologies: A review. *Journal of Environmental Chemical Engineering, 11*(3), Article 109610. https://doi.org/10.1016/j.jece.2023.109610

Wei, T., Zhu, Y., Duan, G., Han, J., Han, X., Zhang, C., & Jiang, S. (2025). Recent advances in nanocellulose-derived materials for dyes adsorption: A review. *International Journal of Biological Macromolecules*. https://doi.org/10.1016/j.ijbiomac.2025.141770

Zeng, W., Loi, Q. K., Shi, J., Liu, L., Liu, M., & Do, D. D. (2024). Understanding water adsorption in hierarchical carbon—The significance of pore connectivity and functional group configurations. *Fuel, 371*, Article 131933. https://doi.org/10.1016/j.fuel.2024.131933

Zhao, W., Hao, C., Guo, Y., Shao, W., Tian, Y., & Zhao, P. (2023). Optimization of adsorption conditions using response surface methodology for tetracycline removal by $MnFe_2O_4$/multi-wall carbon nanotubes. *Water, 15*(13), 2392. https://doi.org/10.3390/w15132392

Publisher's Note Springer Nature remains neutral with regard to jurisdictional claims in published maps and institutional affiliations.